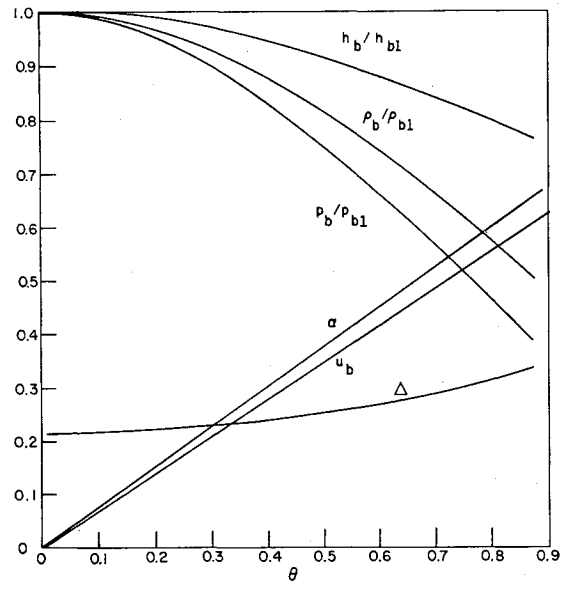

Fig. 2 Flow variable profiles for an ideal gas, $M_\infty = 3.0$, $\gamma = 1.4$.

Values of flow variables on the body and behind the shock on the stagnation streamline are found readily from normal shock conservation relations. With a trial value of Δ_1, Eqs. (14) and (15) can be solved for the unknowns κ and $(d\omega/d\theta)_1$. These quantities directly determine θ^* and $(d\alpha/d\theta)_1$.

The iteration cycle may be described as follows. A trial value of Δ_1 is selected and substituted into Eqs. (14) and (15), giving θ^* and $(d\alpha/d\theta)_1$. Using this θ^*, Eqs. (12) and (13) are solved for α^* and Δ^*. Equation (9) is then used to calculate a corresponding Δ_1. The difference between the assumed value and the value resulting from the calculation cycle becomes the error associated with the trial Δ_1. By iteration, the two values are made to agree to the required degree of accuracy.

III. Applications and Results

Computer programs were prepared using this method and computations accomplished on the UNIVAC LARC computer. The rapidity of these calculations may be emphasized by the fact that solutions for an ideal gas were obtained for twenty Mach numbers from 1.7 to 100, and these solutions listed in both tabular and graphical form in less than 1 min of computer execution time. Figure 2 is a typical result for a freestream Mach number of 3. Figure 3 compares the pressure distribution with that of Belotserkovskii[1] and the experimental results of Baer.[3] Table 1 gives a comparison of detachment distances.

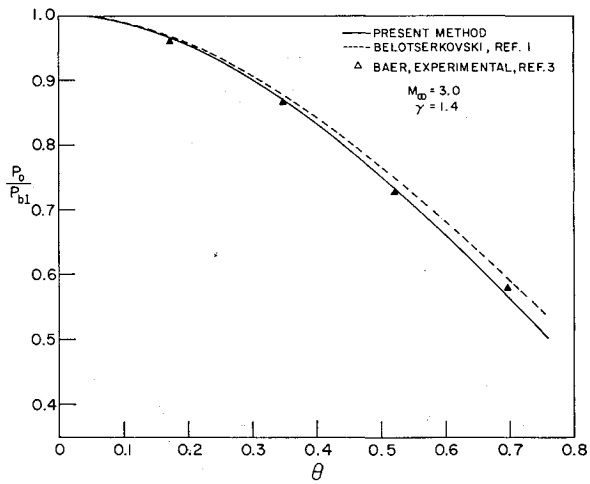

Fig. 3. Pressure distribution on a sphere for an ideal gas.

Table 1 Comparison of shock detachment distance for a spherical body ($\gamma = 1.4$)

M_∞	Present method	Belotserkovskii
1.7	0.472	...
1.8	0.418	...
2.0	0.350	...
2.5	0.260	...
3.0	0.216	0.215
4.0	0.175	0.175
6.0	0.147	0.149
8.0	0.138	...
10.0	0.134	0.136
15.0	0.130	...
20.0	0.128	...
30.0	0.127	...
50.0	0.127	...
100.0	0.127	...
∞	0.127	0.128

This method is readily adaptable to arbitrary equations of state. The solutions strongly depend upon property values behind a normal shock and their stagnation values and upon property values at the sonic point on the body. For an equation of state of the general form

$$p = p(\rho, h) \tag{16}$$

these quantities may be determined readily and the oblique shock conservation equations solved by iteration. For example, the convenient Bade[4] approximation for the equation of state of dissociated air was fitted into these programs and computations readily accomplished.

References

[1] Belotserkovskii, O. M., "The calculation of flow over axisymmetric bodies with a decaying shock wave," Avco Corp. Rept. RAD-TM-62-64 (September 1962).

[2] Hayes, W. D. and Probstein, R. F., *Hypersonic Flow Theory* (Academic Press, Inc., New York, 1959), Chap. VI, p. 202.

[3] Baer, A. L., "Pressure distributions on a hemisphere cylinder at supersonic and hypersonic Mach numbers," Arnold Engineering Development Center, AEDC TN-61-96 (1961).

[4] Bade, W. L., "Simple analytical approximation to the equation of state of dissociated air," ARS J. 29, 298–299 (1959).

Flow Fields about Highly Yawed Cones by the Inverse Method

D. W. Eastman* and M. E. Omar†
The Boeing Company, Seattle, Wash.

Nomenclature

B_s = bluntness parameter
C_p = pressure coefficient
h = altitude
M_∞ = freestream Mach number
R_s = conic radius of curvature at X axis (Fig. 1)
V_∞ = freestream velocity
α = angle of attack
δ = cone half-angle
θ, φ = spherical coordinates

Received March 19, 1965; revision received June 4, 1965.

* Research Engineer, Aerospace Division. Member AIAA.
† Associate Engineer, Applied Mathematics, Aerospace Division.

Subscripts

b = body axis centerline
s = shock axis centerline

Introduction

THIS note shows that the "inverse method" of solution[1] can be used to calculate the inviscid flow field on the windward side of a highly yawed cone traveling at hypersonic speeds. The only limitation is the requirement that the shock wave on the cone be attached.

Stocker and Mauger[2] recently derived equations of motion for the flow around a yawed cone, which are ideal for finite difference numerical solution. However, their solution is difficult to apply because the shock shape around the cone is defined with a Fourier series. An improved method of defining the shock shape is necessary to obtain accurate and prompt results.

Shock-Shape Definition

It was found that the shock shape for a blunt body could be represented by the equation for a conic.[3] It was assumed that the cross-sectional shape of the shock wave on the windward side of the cone also could be represented by the equation for a conic (Fig. 1)

$$Y^2 = 2R_sX - B_sX^2 \tag{1}$$

Equation (1) must be transformed to the spherical coordinate system used by Stocker and Mauger. From the geometry of Fig. 1

$$\begin{aligned} X &= \tan\theta_{\varphi_s=0} - \tan\theta\cos\varphi_s \\ Y &= \tan\theta\sin\varphi_s \\ R_s &= \tan\theta_{\varphi_s=0} \end{aligned} \tag{2}$$

where the axial length of the cone is taken as unity. Substituting Eqs. (2) into Eq. (1)

$$\tan\theta = \tan\theta_{\varphi_s=0}\{(B_s - 1)\cos\varphi_s + [(B_s - 1)^2\cos^2\varphi_s + (2 - B_s)(\sin^2\varphi_s + B_s\cos^2\varphi_s)]^{1/2}\}/(\sin^2\varphi_s + B_s\cos^2\varphi_s) \tag{3}$$

Equation (3) is the equation for the shock shape in spherical coordinates with three unknowns $\theta_{\varphi_s=0}$, B_s, and α_s.

Method of Solution

The method of calculating the shock layer flow will be described only briefly, as it is fully documented in Ref. 4. After estimating $\theta_{\varphi_s=0}$, B_s, and α_s, Eq. (3) is used to define the shock shape on the windward side of the cone, and the Rankine shock equations are solved to obtain flow conditions behind the shock. The transformed equations of motion[2] are then integrated toward the body until it is reached. If the body shape is not the one desired, a new shock shape estimate is made, and the calculation is repeated until the correct body is obtained.

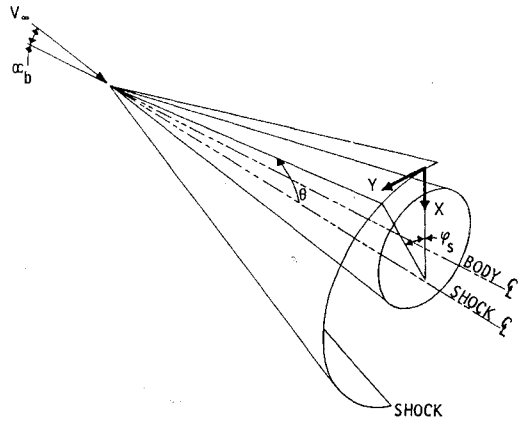

Fig. 1 Coordinate system.

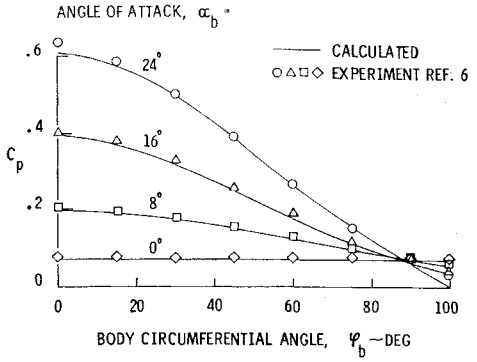

Fig. 2 Comparison of calculated and experimental pressure coefficients on the cone surface; $M_\infty = 7.95$ and $\delta = 10°$.

Although no singularities were encountered and the method of solution appears simple, the following two difficulties remain: 1) a finite difference solution of the equations of motion tends to become unstable unless special numerical techniques are used, and 2) it is difficult to obtain the body shape without interrupting the calculation and examining results. It is preferable to complete the calculation in an uninterrupted series of computer calculations, i.e., obtain the body shape, compare it with the desired body shape, estimate a new shock shape, and repeat the flow field calculations until a satisfactory solution is obtained. The lengthy solutions to these problems are discussed in Ref. 4.

Results

In order to verify the method of solution and the assumption that the shock could be represented by the equation for a conic, calculated results were compared with existing experimental and theoretical data. Theoretical results were compared with experimental data obtained by Tracy[6] for a 10° half-angle cone tested in air at $M_\infty = 7.95$. Because the total temperature for the tests was 1360° Rankine, a perfect gas with $\gamma = 1.4$ was assumed for the calculations. Figure 2 shows the excellent comparison of calculated and experimental surface pressures at several angles of attack. Figures 3 and 4 show a comparison of calculated and experimental shock-shape parameters. The difference between experimental and theoretical results is primarily due to a systematic shock-shape measurement error by Tracy. Since the error is systematic, the experimental results are still useful.

Flow fields for a 10° cone at $V_\infty = 18{,}000$ fps and 50,000-ft altitude were calculated for angles of attack to 60° using the real air model proposed by Hansen.[5] Figure 4 shows the variation of the shock-shape parameters with angle of attack. The fluctuations in the curves of $(\alpha_b - \alpha_s)$ and $(\theta_{\varphi_s=0} - \delta)$ are thought to be due to real gas effects in the shock layer.

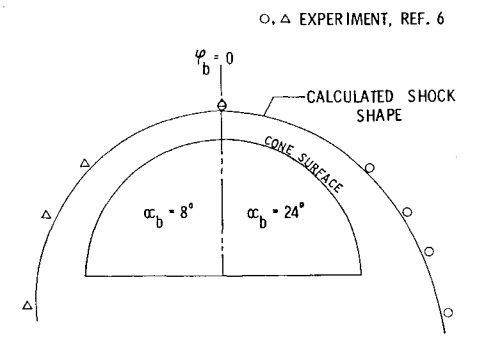

Fig. 3 Comparison of calculated and experimental shock shapes: $M_\infty = 7.95$ and $\delta = 10°$.

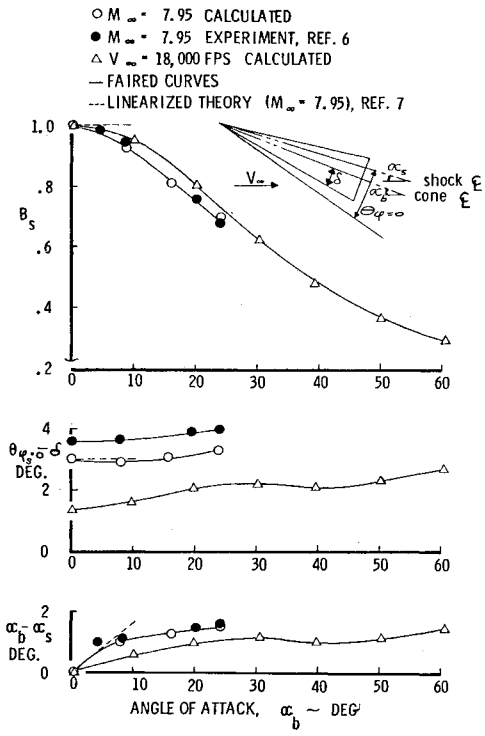

Fig. 4 Comparison of calculated and experimental shock shape parameters: $\delta = 10°$.

Figure 5 shows lines of constant temperature, density, entropy, and pressure in the windward shock layer of the cone at an angle of attack of 60°.

The shock-shape parameters plotted in Fig. 4, as well as additional results not presented here, indicate the following:

1) The difference between the body and shock wave angle of attack ($\alpha_b - \alpha_s$) is small, so that once the desired body angle of attack is specified the shock angle of attack can be accurately estimated. Thus, B_s and $\theta_{\varphi_s=0}$ are essentially the only unknowns that must be estimated to define the shock shape.

2) $\theta_{\varphi_s=0}$ does not vary rapidly with angle of attack. The value for zero angle of attack can be used as an initial estimate.

3) At zero angle of attack the shock shape is circular and therefore, $B_s = 1$. With increasing angle of attack the shock shape becomes more elliptical, and the value of B_s decreases. (B_s was found always to have the same general variation, so that after gaining some experience accurate values could easily be estimated.)

For all results, the assumption that the shock shape could be estimated by the equation for a conic was found to be valid.

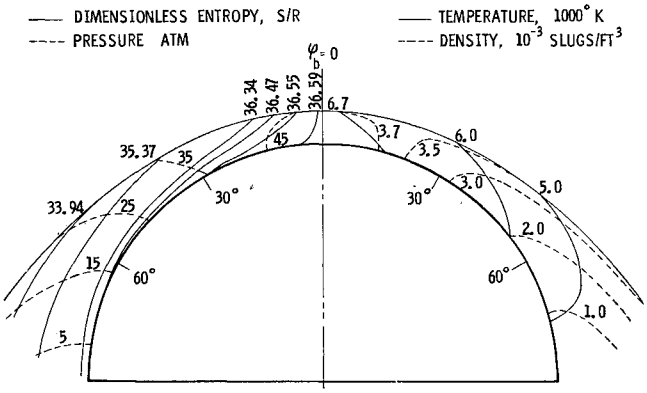

Fig. 5 Variation of shock layer properties for a 10° half-angle cone at 60° angle of attack: $V_\infty = 18{,}000$ fps and $h = 50{,}000$ ft.

References

[1] Hayes, W. D. and Probstein, R. F., "Hypersonic flow theory," (Academic Press, New York, 1959), p. 230.

[2] Stocker, P. M. and Mauger, F. E., "Supersonic flow past cones of general cross-section," J. Fluid Mech. **13**, 383–399 (1962).

[3] Van Dyke, M. D. and Gordon, H. D., "Supersonic flow past a family of blunt axisymmetric bodies," NASA TR R-1 (1959).

[4] Eastman, D. W., "Real gas flow fields about highly yawed cones by the inverse method," Boeing Co. Doc. D2-20447-1 (1964); available through the Defense Documentation Center AD 450 287.

[5] Hansen, C. F., "Approximations for the thermodynamic and transport properties of high-temperature air," NASA TR R-50 (1959).

[6] Tracy, R. R., "Hypersonic flow over a yawed circular cone," Guggenheim Aeronautical Laboratories, California Institute of Technology, GALCIT Memo. 69 (1963).

[7] Sims, J. L., "Tables for supersonic flow around right circular cones at small angles of attack," NASA SP-3007 (1964).

A Random Signal Multiplier for Turbulence Measurements

V. Kruka*

Syracuse University, Syracuse, N. Y.

In the study of turbulent diffusion of a scalar quantity such as temperature it is of interest to investigate correlations of velocity-temperature fluctuations. These correlations are necessary for balancing the perturbed energy and higher order temperature correlation equations. The latter is obtained by multiplying the turbulent energy equation by the temperature fluctuations and averaging over time. The result gives a relation between convection, production, and dissipation of temperature fluctuations. The double correlations found in the energy equation are easily determined by conventional means. The higher order temperature correlation equation, however, gives rise to triple correlations such as $<\theta^2 u_i>$, where θ and u_i represent temperature and velocity fluctuations, respectively. It is for the evaluation of these quantities that the random signal multiplier was designed.

Physically, these correlations are measured by means of a 3-wire hot-wire probe, with the wires placed in the usual X-array but with two wires parallel to each other. For temperature fluctuation measurements one of the parallel wires is at an overheat ratio, the ratio of hot to cold resistance, different from the others. The various mean voltage products $<e_i e_j e_k>$ obtained from the three wires determine the desired double and triple correlations. Often, for the purpose of temperature fluctuation measurements, it has been customary to assume that a wire at a low overheat ratio behaves as a resistance thermometer, whereas one at a high overheat ratio responds only to velocity changes. The errors introduced with this assumption are not always negligible. For instance, in the case of tungsten wires, with an upper practical overheat ratio limit of 1.8, subjected to 10% turbulence and 2°F rms temperature fluctuation, 20% of the signal from the wire is due to temperature effects. Platinum wires with their inherently higher possible overheat ratios will improve but not avoid the approximation. The multiplier removes this source of error by allowing for sensitivity to both velocity and temperature on all wires.

A schematic circuit diagram of the random signal multiplier discussed here is shown in Fig. 1. The device is based

Received June 8, 1965. This work was supported by the National Science Foundation under Grant No. GP-354.

* Research Associate, Department of Mechanical and Aerospace Engineering.